Papers, volume 5 - 1997-2000

Thoft-Christensen, Palle

Publication date:
2006

Document Version
Publisher's PDF, also known as Version of record

CHAPTER 106

WIND TUNNEL TESTS OF A BRIDGE MODEL WITH ACTIVE VIBRATION CONTROL [1]

H.I. Hansen*, P. Thoft-Christensen*, P.A. Mendes** & F.A. Branco**
*University of Aalborg, Aalborg, Denmark
**University of Lisbon, Lisbon, Portugal

SUMMARY

The application of active control systems to reduce wind vibrations in bridges is a new area of research. This paper presents the results that were obtained on a set of wind tunnel tests of a bridge model equipped with active movable flaps. Based on the monitored position and motion of the deck, the flaps are regulated by a control algorithm so that the wind forces exerted on them counteract the deck oscillations.

1. INTRODUCTION

The tendency to increase the span length of cable-stayed and suspension bridges has increased the importance of wind effects on such structures, and it often occurs that the aerodynamic issues are crucial to the design. The accidents that have occurred in bridges due to wind led to a significant amount of research in this area and, nowadays, the design of important bridges involves both numerical model-based and wind tunnel studies to achieve structural solutions that are not wind-sensitive.

In addition to the problems that may arise from aerodynamic instability, several bridges also present large-amplitude vibrations even under moderate wind speeds, which lead to their frequent closing to traffic with the associate social and economical inconvenient.

In order to solve mainly this second type of problems, a new strategy is being investigated by the scientific community; see Hansen & Thoft-Christensen [1] and Kwon, Chang & Kim [2]. This strategy consists on the installation of active control systems that are activated under wind vibration situations, in order to reduce the

[1] Structural Engineering International, Vol. 10, No. 4, 2000, pp. 249-253.

vibration levels and guarantee the serviceability conditions of the structure.

This paper presents the results from a campaign of wind tunnel tests that were performed for a bridge model equipped with active movable flaps; Hansen [3]. The idea for this control system (Ostenfeld & Larsen [4], European Patent Specification [5] was based on damping the oscillations of the deck through the forces exerted on the flaps by the wind; see figure 1. Based on the monitored position and motion of the deck, the flaps are regulated by a control algorithm so that the wind forces exerted on them counteract the deck oscillations.

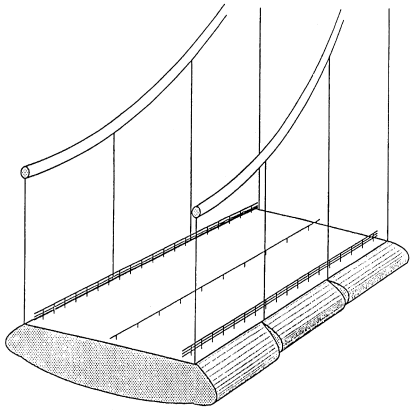

Figure1: Flaps on a bridge girder

In real bridges these flaps will be divided into segments along the span. Each segment may then be regulated independently and it is expected that these flaps do not need to be mounted over the entire span of the bridge.

2. WIND TUNNEL TESTS

The tests were performed in a wind tunnel of the open return type. A contraction unit 3.00m long (with a length: with ratio of 5.44: 1) takes the air to the test chamber, which has a cross section 1.50 m × 1.50 m (at the entrance) and is 5.00 m long. After the test chamber, there is a diffuser to make the transition from the square shape to a circular duct, 1.80 m diameter, where the fan is located.

The fan is of the variable pitch type and works at a constant speed of rotation (1470 rpm). The pitch is controlled manually by a compressed air system. The maximum wind speed inside the test section is 40m/s. The wind speed is measured by using a Pitot-Prandtl tube connected to a pressure transducer.

3. BRIDGE MODEL

Figure 2 illustrates the cross section of the model that was tested. The width of the model excluding the flaps is denoted by *B′* and the height of the model is 0.15 *B′*. The width of each flap is 0.25 *B′*, so that the total width (*B*) is equal to 1.50 *B′*.

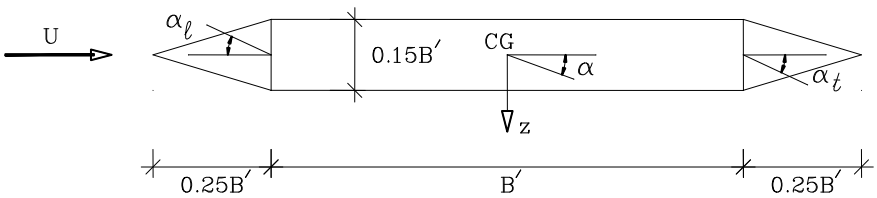

Figure 2: Cross section of the model (B' = 625mm)

The model was made as light as possible, as the part of the regulation system to be fixed inside the model (namely two servo motors and two reduction gears) is relatively heavy. Thus, the model was made of foam with an aluminium frame to make it stiff. This frame was provided with holes where possible, to reduce its weight. The

space between the model and the flaps was closed by a piece of fabric, in order to prevent the flow from being separated in this region (figure 3).

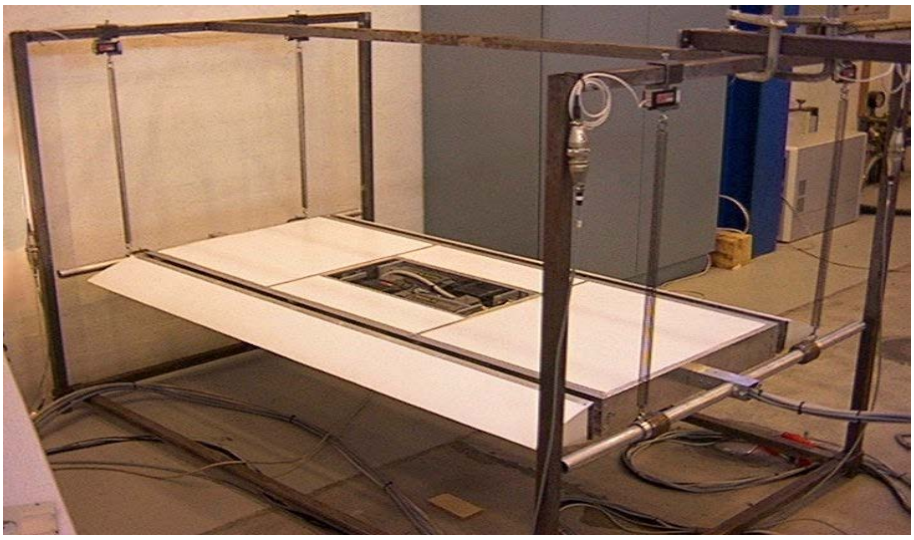

Fig. 3: View of the model

The model was 1480mm long and was connected in each side to a horizontal extension rod. Each rod was connected to an arm with dummy masses, in order to represent the correct mass and mass inertia. The arms were suspended in each side by helical springs that could be moved along the arm in order to adjust the torsional frequency.

During the experiments the motion of the model was measured by four load cells. The movements in the wind direction were prevented by using long drag wires attached to the steel frames. Figure 4 illustrates the model in the wind tunnel.

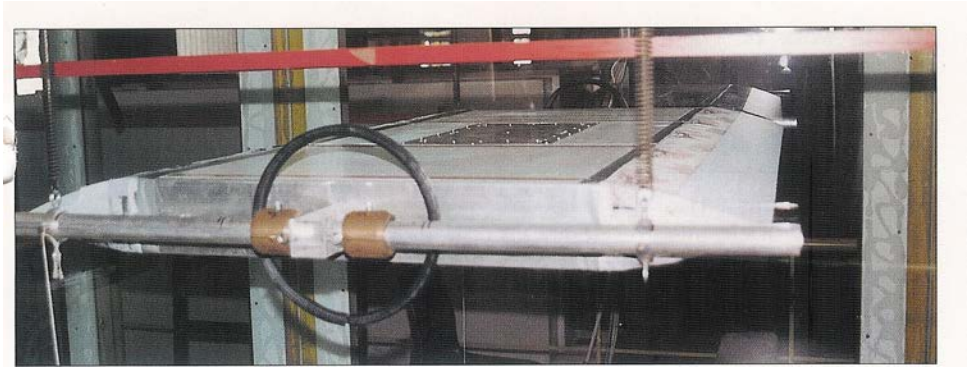

Fig. 4: Testing in the wind tunnel

The scales adopted for the experiments were: λ_L = 1:40 (length), λ_V = 1:4 (velocity) and λ_ρ = 1 (mass density). Based on these fundamental values, the frequency scale is $\lambda_f = \lambda_V / \lambda_L$ = 10:1 and the mass per unit length scale, for instance, is $\lambda_\mu = \lambda_\rho (\lambda_L)^2$ = 1:1600. The values assumed for the prototype and the corresponding values for the model are shown in Table1.

Characteristic	Prototype (assumed values)	Model (theoretical values)
Width of the deck (B')	25 m	0.625 m
Total width (B)	37.5 m	0.9375 m
Mass per unit length (with no flaps)	25 000 kg/m	15.625 kg/m
Mass per unit length of each flap	1160 kg/m	0.725 kg/m
Mass moment of inertia per unit length	2.1 10^6kgm	0.820 kgm
First eigenfrequency (bending)	0.08 Hz	0.80 Hz
Second eigenfrequency (torsion)	0.16 Hz	1.60 Hz

Table 1: Characteristics assumed for the prototype and corresponding model values

The critical wind speed for coupled flutter in a flat plate (U_{cr}) may be estimated by the Selberg's formula:

Error! (1)

where μ and I are the mass properties per unit length, f_Z and f_a are the frequencies of oscillation and ρ is the volume mass of the air.

The values assumed for the prototype and for the velocity scale were chosen in order to get a flutter wind speed around 10 m/s, which is a value easily attainable in the wind tunnel. If the values assumed for the prototype are considered, namely B = 37.5 m, I= 2.1×10^6 kg.m/m, μ = 27320kg/m, f_Z = 0.08 Hz and f_a = 0.16 Hz, along with ρ = 1.28 kg/m^3, the then U_{cr} =36.4 m/s. Thus, with λ_V = 1:4, the expected flutter wind speed in the tunnel is U_{cr} =9.1m/s.

Considering the length of the model (1.48 m) and the values shown in Table 1, the theoretical value of the total oscillating mass is M = 25.271 kg. Thus, in order to get the desired frequency for the vertical motion (f_V = 0.80Hz), the four helical springs were ordered with a stiffness k given by:

$$f_v = \frac{1}{2\pi}\sqrt{\frac{4k}{M}} \quad \Leftrightarrow \quad k = \frac{M\left(2\pi f_v\right)^2}{4} = 160\ N/m \tag{2}$$

4. FLAP REGULATION SYSTEM

The regulation system to move the flaps consists of two servo systems, the regulation software to position the flaps and the control software to calculate the desired position of the flaps.

Each servo system consists of a servo amplifier, a servo motor and a reduction gear. Two servo systems are used as the flaps are regulated independently. The servo amplifiers are placed outside the model, while the servo motors and the reduction gears are fixed inside the model. Each reduction gear is connected to a flap via cables. The position regulator is basically a proportional derivative (PID) regulator in the servo amplifier.

During the experiments the flaps can only be regulated by the software, i.e., there is no manual control. If the flaps turn too much, with risk of damaging the model, the power to the motors may be cut off by switches placed in the model.

5. CALIBRATION OF THE MODEL

The total mass of the model after construction, including flaps, was measured as 26.553kg (i.e. μ=17.94 kg/m). This value is only 5% above the theoretical one (25.271kg) and so the consequences of this difference were disregarded. With respect to the eigenfrequencies, the mean value for the vertical motion was 0.83 Hz (versus a desired value of 0.80Hz) and for the torsional motion the value 1.61 Hz was obtained (versus 1.60Hz) with the distance between the springs (2*a*) being equal to 704mm.

Based on these results, the global stiffness of the model in bending and in torsion (denoted by k_z and k_a respectively) and its equivalent mass moment of inertia per unit length were estimated through the following expressions:

$$k_z = \left(2\pi f_z\right)^2 \mu = 488 \text{ N/m}^2 \tag{3}$$

$$k_a = a^2 k_z = 60.5 \text{ N} \tag{4}$$

$$I = \frac{k_a}{\left(2\pi f_a\right)^2} = 0.590 \text{ kgm} \tag{5}$$

The values measured for the structural damping ratio in bending $\left(\zeta_z\right)$ and in torsion $\left(\zeta_a\right)$ were 1.2% and 0.8%, respectively.

If the theoretical flutter derivatives of a flat plate are considered along with this set of experimental values, the corresponding coupled flutter wind speed $\left(U_{cr}\right)$ is 8.18 m/s. Although the Selberg's formula does not take into account the real values of damping, it usually provides a good estimate of U_{cr} if $f_a / f_z > 1.50$. In this case, the Selberg's formula leads U_{cr} = 8.5 m/s. This order of magnitude of the critical wind speed was in fact observed in the wind tunnel in the case of fixed flaps (configuration 0).

6.EXPERIMENTAL RESULTS

The main purpose of the first set of wind tunnel experiments was to investigate how the effective damping of the model depends on the flap configuration for variable wind velocities. Thus, for simplicity, the initial tests were performed with the two flaps moving with the same phase angle, which is not an optimal solution. With this simple control algorithm, the desired angles of the trailing and leading flaps (α_t and α_l, respectively) are given through:

$$\alpha_t\left(t\right) = a_t \alpha\left(t\right) \tag{6}$$

$$\alpha_l\left(t\right) = a_l \alpha\left(t\right) \tag{7}$$

where a_t and a_l are amplitude amplification factors and $\alpha\left(t\right)$ is the torsional angle exhibited by the model at time *t*. The following configurations were tested:

- configuration 0: α_t = a_l = 0;
- configuration 1: α_t = -6; α_l = 6
- configuration 2: α_t = -20; α_l = 20
- configuration 3: α_t = 6; α_l = -6
- configuration 4: α_t = 20; α_l = -20.

For each configuration both the vertical and the torsional motions were recorded within a range of wind speed. All the experiments were repeated 3-5 times. The flaps were started slowly by multiplying the desired positions by a factor t/t_0, when $t < t_0$. The value t_0=1s was considered.

During a damping experiment the following parameters were stored every 12 ms:

- the displacements of the model (vertical z and torsional α)
- the specified angle of the trailing and leading flap (α_t and α_l)
- the actual angle of the trailing and leading flap (α_{ta} and α_{la}).

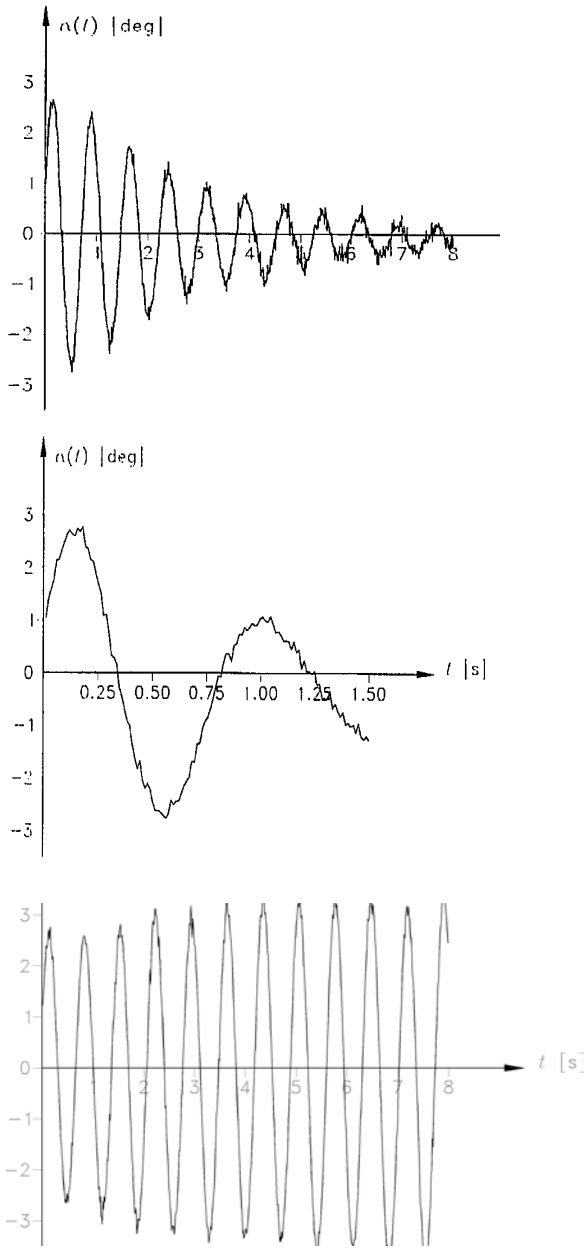

Figure 5: Torsional motion for different flap configurations (U = 6.1 m/s)

Figure 5 illustrates the torsional motion for a wind speed of 6.1m/s and for the flap configurations 0, 2 and 4. The results clearly show that, on one hand, the global damping of the oscillations can be rather increased (configuration 2); on the other hand,

it is possible to make the flap configuration very unfavourable (e.g. configuration 4) so that flutter occurs at a lower wind speed than with no flaps moving. The *t*-axis scale in Figure 5.b is different from the scale in Figures 5.a and 5.c because the torsional oscillations with the configuration 2 decayed rapidly to zero as a result from a very high effective damping.

The measurements were noisy and therefore they were filtered in order to estimate the circular frequency and damping ratio. A second-order filter was used to filter the noisy position measurements after the experiments. This filter is defined by:

$$u_f(k) = epu_f(k-1) - p^2 u_f(k-2) + (1-p)^2 u(k) \tag{8}$$

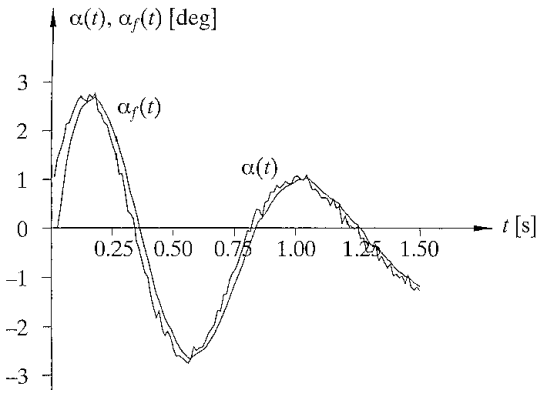

Fig. 6: Measured and filtered torsional motion for flap configuration 2

where $u(k)$ is the noisy measurement at time step *k*, $u_f(k)$ is the filtered value and *p* is the pole. If $p = 0$, the filtered values are equal to the measured values; if $p = 1$, the filtered values do not depend on the measured values. A value of $p = 0.5$ was selected for all the experiments. Figure 6 illustrates the measured torsional motion and the corresponding filtered motion for flap configuration 2 and $U = 6.1$ m/s.

The damping ratio for torsional motion was estimated from the experiments by Hilbert transformation of the filtered time series and is shown in Figure 7 as a function of wind speed. It might be seen that when the flap configurations 1 and 2 are used the global damping ratio is increased, and that when the flap configurations 3 and 4 are used the global damping ratio is decreased. The effectiveness of the flaps could not be shown for wind speeds above the critical one.

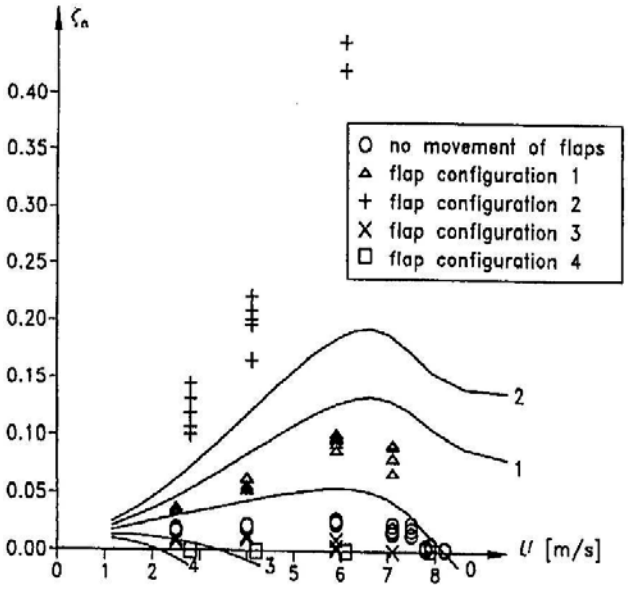

Configuration	a_t	a_l
0	0	0
1	1.9	2.0
2	3.4	3.6
3	2.0	2.0
4	3.4	3.6

Fig. 7: Theoretical (solid lines) and experimental values of the damping ratio for torsional motion.

7. EXPERIMENTAL VERSUS THEORETICAL RESULTS

It is common practice to admit that the motion-induced wind loads on the cross section of a bridge deck depend linearly on the displacements of the deck and on their first time derivatives. This hypothesis comes from the pioneering work of Theodorsen on the behavior of thin airfoils in incompressible flow.

In the field of Bridge Aerodynamics, assuming that both the vertical displacements (*z*) and the rotations (α) of the deck are harmonic (with circular frequency ω), it is usual to work with the following format:

$$L_a = \frac{1}{2}\rho U^2 B\left[KH_1^*(K)\frac{\dot{z}}{U} + KH_2^*(k)\frac{B\dot{\alpha}}{U} + K^2 H_3^*(K)\alpha + K^2 H_4^*(K)\frac{z}{B}\right] \quad (9)$$

$$M_a = \frac{1}{2}\rho U^2 B\left[KA_1^*(K)\frac{\dot{z}}{U} + KA_2^*(k)\frac{B\dot{\alpha}}{U} + K^2 A_3^*(K)\alpha + K^2 A_4^*(K)\frac{z}{B}\right] \quad (10)$$

where L_a and M_a are the motion-induced lift and torsional moment, $K = B\omega/U$ is the so-called reduced frequency and the coefficients $H_1^* - H_4^*$ and $A_1^* - A_4^*$ are aerodynamic derivatives.

The theoretical expressions for the aerodynamic derivatives of a thin airfoil (with no flaps) are well known (see Simiu & Scanlan [6]). Based on the principles of potential flow theory, work has been extended his work to the case of a trailing flap on a thin airfoil. Assuming that the rotation of the leading flap has no effect on the circulation, it can be shown that of a thin airfoil with a leading flap and a trailing flap, both oscillating with the same frequency than the flat plate, the equations 9 and 10 still apply with a proper redefinition of the flutter derivatives H_2^*, H_3^*, and A_3^*: see Hansen [3].

The theoretical and experimental values of the damping ratios and of the circular frequencies for the torsional motion with the flap configurations 0-4 are shown in Figures 7 and 8. The values shown correspond to the average of the values that were obtained in the experiments performed for each configuration (3 to 5 repetitions).

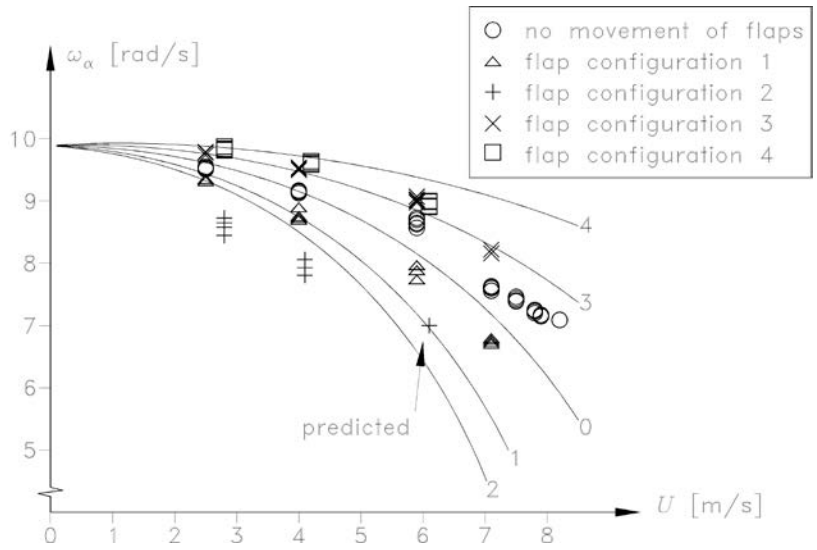

Fig. 8: Theoretical (solid lines) and experimental values of the circular frequency for torsional motion

The estimated frequencies generally follow the theoretical curves for wind velocities below 5m/s, except for case 2 where the deviations can be caused by the relatively short time series that were recorded (due to the high effective damping). The experimental damping ratio is smaller for cases 0 and 1 than the theoretical damping ratio but the curve is almost the same. In case 2 the experimental damping is much greater than the theoretical one.

8. PROBLEMS FOUND DURING THE EXPERIMENTS

During the preparation of the wind tunnel tests some unanticipated problems were found, namely:

- noisy measurements of the displacements from the load cells, partly due to the servo motors;
- occurrence of longitudinal (standing) waves in the springs;
- static divergence of the model at a low wind velocity, close to the flutter velocity in configuration 0 (i.e. around 8.5 m/s).

The noisy measurements were dealt with by decreasing the value of P in the PID-regulator, so that the servo motors react slowly and become little sensible to noise.

The occurrence of static divergence limited the range of test velocities in the wind tunnel and was not anticipated in the design of the model, as the attention was focused on flutter. If a simple two-dimensional approach to the divergence phenomenon on a bridge deck had been considered, the divergence velocity (U_d) would have been estimated through [6]:

$$U_d = \sqrt{\frac{2k_a}{\rho B^2 \frac{dC_M}{da}}} \tag{11}$$

where C_M is the torsional moment coefficient of the section. Considering that for an ideal flat plate $dC_M / d\alpha = \pi / 2$, k_a = 60.5 N, B = 0.937 m and ρ = 1.28 kg/m^3, then U_d = 8.3 m/s. This value is similar to the flutter velocity in configuration 0 and such a velocity was observed during the experiments.

9. CONCLUSIONS

A series of wind tunnel tests was performed for a simplified model of a bridge deck equipped with movable flaps regulated actively. Experiments were performed for the model without moving the flaps and with four moving flap configurations, two of them favourable and the other two unfavourable. The phase angle was kept constant during the experiments.

The results obtained show that it is possible to reduce the oscillations and to prevent aerodynamic instabilities using this technique. The damping ratio depends on the wind speed and on the flap configuration, and it may increase considerably even for non-optimal flap configurations. On the other hand, if the movement of the flaps is not regulated properly, then the oscillations may increase as well, with the occurrence of flutter at rather low wind speeds.

The damping and frequency parameters estimated from the wind tunnel experiments are compared with the theoretical parameters, predicted by extending the Theodorsen theory to a thin airfoil with leading and trailing edges. The effective

frequencies measured during the tests follow the theoretical trend. The estimated damping values did not fit so well with the theoretical values, but similar trends were also obtained.

ACKNOWLEDGEMENTS

This research was supported by the Instituto de Cooperação Científica e Tecnológica Internacional and by the Danish Technical Research Council.

REFERENCES

[1] Hansen, H. & Thoft-Christensen, P. Active control of long bridges using flaps. Proc. of Second World Conf. on Structural Control, Kyoto, 1998.

[2] Kwon, Y., Chang, S. & Kim,. Active suppression of flutter and gust response of bridges using edge control surfaces. Proc. of 10th Int. Conf. on Wind Engineering, Copenhagen, 1999, pp. 941-946.

[3] Hansen, H. Active vibration control of long suspension bridges, Ph.D. Thesis, Aalborg University, 1998.

[4] Ostenfeld, K. & Larsen, A. Elements of active flutter control of bridges. Proc. of New Technologies in Structural Engineering, LNEC, Lisbon, 1997, pp. 683-694.

[5] European Patent Specification. A system and a method of counteracting wind induced oscillations in a bridge girder. EP 0 627 031 B1. Bulletin 1996/24.

[6] Simiu, E. & Scanlan, R. Wind effects on structures. Fundamentals and applications to design, John Wiley & Sons, 3rd edition, New York, 1996.